The Multi-cover Persistence of Euclidean Balls*

Herbert Edelsbrunner and Georg Osang

IST Austria (Institute of Science and Technology Austria), Am Campus 1, 3400 Klosterneuburg, Austria, edels@ist.ac.at, georg.osang@ist.ac.at

Abstract

Given a locally finite $X \subseteq \mathbb{R}^d$ and a radius $r \geq 0$, the *k-fold cover* of X and r consists of all points in $\mathbb{R}^d$ that have k or more points of X within distance r. We consider two filtrations — one in *scale* obtained by fixing k and increasing r, and the other in *depth* obtained by fixing r and decreasing k — and we compute the persistence diagrams of both. While standard methods suffice for the filtration in scale, we need novel geometric and topological concepts for the filtration in depth. In particular, we introduce a rhomboid tiling in $\mathbb{R}^{d+1}$ whose horizontal integer slices are the order-k Delaunay mosaics of X, and construct a zigzag module from Delaunay mosaics that is isomorphic to the persistence module of the multi-covers.

Keywords and phrases: Delaunay mosaics, hyperplane arrangements, discrete Morse theory, zigzag modules, persistent homology.

1 Introduction

The work in this paper is motivated by density fluctuations in point configurations. These fluctuations can be large — and the task may be the identification of regions with a prescribed density profile — or they can be small — and the goal may be to pick up subtle variations. For example, we may want to quantify local defects in lattice configurations or describe long-range differences between similar configurations, such as the *face-centered cubic* (FCC) lattice and the *hexagonal close-packed* (HCP) configuration in $\mathbb{R}^3$. Using standard methods from computational geometry and topology, we describe mathematical and computational tools to quantify density fluctuations. Our work is closely related to the *distance to a measure* introduced in [6]. As demonstrated in a follow-up paper [14], this distance can be approximated using the *order-k Voronoi tessellation* of the configuration, a concept introduced in the early days of computational geometry [20], but see also [11, 16]. Order-k Voronoi tessellations are also at the core of our work:

1. Given a locally finite set $X \subseteq \mathbb{R}^d$, we introduce a rhomboid tiling in $\mathbb{R}^{d+1}$ whose horizontal slices at integer depths are the geometric duals of the order-k Voronoi diagrams.

We call these duals the *order-k Delaunay mosaics* of X. The tiling clarifies the structure of individual mosaics and the relationship between them. Restricting the order-k Voronoi tessellation to the *k-fold cover* of the balls with radius $r \geq 0$ centered at the points in X, we get a subcomplex of the order-k Delaunay mosaic; see [15] for the introduction of this concept for statistical purposes in two dimensions. Our second result makes use of the family of such subcomplexes obtained by varying the scale:

2. Fixing k and varying r, we compute the persistence diagram of the density fluctuations from the filtration of order-k Delaunay mosaics of X.

* This work is partially supported by the DFG Collaborative Research Center TRR 109, 'Discretization in Geometry and Dynamics', through grant no. I02979-N35 of the Austrian Science Fund (FWF).

The ingredients for our second result are standard, but to get the actual results, we needed an implementation of the order-k Delaunay mosaic algorithm, which we developed based on the rhomboid tiling. In contrast to [2, 19], this gives a simple implementation, which we will describe elsewhere. Using this software in $\mathbb{R}^3$, we find that the FCC and the HCP configurations have the same persistence diagram for $k = 1, 2, 3$ but different persistence diagrams for $k = 4, 5$. Our third result is an algorithm for the persistence of the multi-covers obtained by varying the depth:

3. Fixing r and varying k, we compute the persistence diagram of the filtration of multi-covers of X.

Several innovative adaptations of the standard approach to persistence are needed to get our third result. The main challenge is the combinatorial difference of the Delaunay mosaics from one value of k to the next. Here we use again the rhomboid tiling to establish a zigzag module whose persistence diagram is the same as that of the filtration of multi-covers. We get the persistence diagram using the algorithm in [4, 5]. Our work is also related to the study of multi-covers based on Čech complexes in [21]. While the relation between the different Čech complexes is simpler than that between the Delaunay mosaics, their explosive growth for increasing radius leads to algorithms with prohibitively long running time.

Outline. Section 2 describes the rhomboid tiling in $\mathbb{R}^{d+1}$ that encodes the Delaunay mosaics of all orders of a locally finite set in $\mathbb{R}^d$. Section 3 relates the k-fold covers with the order-k Delaunay mosaics and introduces radius functions on the rhomboid tiling and the mosaics. Section 4 introduces slices of a tiling at half-integer depths and explains how they are used to compute the persistence diagram in depth. Section 5 concludes the paper.

2 Rhomboid Tiling

Given a locally finite set in $\mathbb{R}^d$, we are interested in the collection of Delaunay mosaics of all orders. Assuming the set is in general position, there exists a rhomboid tiling in $\mathbb{R}^{d+1}$ such that the Delaunay mosaics are horizontal slices of the tiling. This section introduces the tiling and proves the relation to Delaunay mosaics.

Rhomboid tiling. Let $X \subseteq \mathbb{R}^d$ be locally finite and in general position. We say a point $x \in X$ lies *inside* a $(d-1)$-dimensional sphere, S, if it belongs to the open ball bounded by S, and x is *on* the sphere if $x \in S$. We write $\text{In}(S), \text{On}(S) \subseteq X$ for the points inside and on S, respectively, and we call $(I, U) \in 2^X \times 2^X$ a *spherical pair* if there exists a sphere with $I = \text{In}(S)$ and $U = \text{On}(S)$. By assumption of general position, we have $0 \leq |U| \leq d+1$, but there is no a priori upper bound on the size of I. We call $(\emptyset, \emptyset)$ the *empty spherical pair*.

We map each spherical pair to a parallelepiped in $\mathbb{R}^{d+1}$, which we call the *rhomboid* of the pair, denoted $\text{rho}(I, U)$. To define it, we write $y_x = (x, -1) \in \mathbb{R}^{d+1}$, for every $x \in X$, and $y_Q = \sum_{x \in Q} y_x$ for every $Q \subseteq X$. The $(d+1)$-st coordinate of y_Q is therefore $-|Q|$, and we call $|Q|$ the *depth* of the point. With this notation, $\text{rho}(I, U) = \text{conv}\,\{y_Q \mid I \subseteq Q \subseteq I \cup U\}$. The rhomboid is *anchored* at the vertex with least depth, which is y_I, and it is spanned by the vectors y_x, with $x \in U$. Its dimension is the number of vectors, which is $\dim \text{rho}(I, U) = |U|$. Observe that every face of a rhomboid is again the rhomboid of a spherical pair. To see this, we note that each face of $\text{rho}(I, U)$ can be written as $\text{rho}(I \cup U_{in}, U_{on})$ in which $U = U_{in} \cup U_{on} \cup U_{out}$ is a three-partition of U. Indeed, there is a bijection between the faces of the rhomboid and the three-partitions. By definition, the *rhomboid tiling* of X, denoted $\text{Rho}(X)$, is the collection of all rhomboids defined by spherical pairs; see Figure 1.

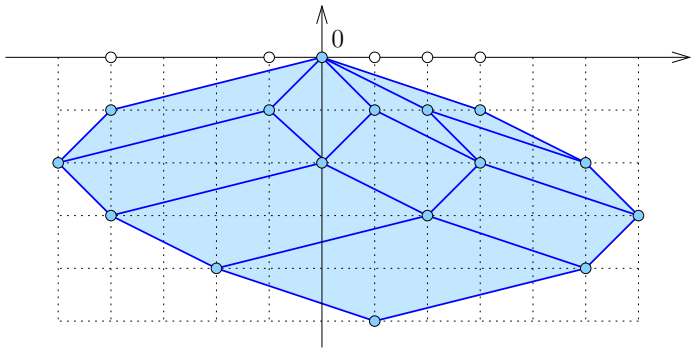

Figure 1 The rhomboid tiling of 5 points on the real line. The horizontal line at depth k intersects the tiling in a geometric realization of the order-k Delaunay mosaic of the 5 points.

As suggested by the figure, the empty spherical pair is mapped to the origin of $\mathbb{R}^{d+1}$. We claim the following properties.

▶ **Theorem 1** (Rhomboid Tiling). *Let $X \subseteq \mathbb{R}^d$ be locally finite and in general position. Then*
1. $\mathrm{Rho}(X)$ *is dual to an arrangement of hyperplanes in $\mathbb{R}^{d+1}$;*
2. $\mathrm{Rho}(X)$ *is the projection of the boundary of a zonotope in $\mathbb{R}^{d+2}$;*
3. *the horizontal slice of* $\mathrm{Rho}(X)$ *at depth k is the order-k Delaunay mosaic of X.*

Note that Claim 2 in Theorem 1 implies that the rhomboid tiling is a geometric realization of the dual of the arrangement in $\mathbb{R}^{d+1}$, that is: its rhomboids intersect in common faces but not otherwise. The remainder of this section proves the first and the last claim, and we omit the proof of the second claim. To keep the proofs self-contained, we will define hyperplane arrangements and order-k Delaunay mosaics before we use them. We refer to [7] for additional information on their relation to point configurations.

Proof of Claim 1: hyperplane arrangement. For each point $x \in X$, write $f_x \colon \mathbb{R}^d \to \mathbb{R}$ for the affine map defined by $f_x(p) = \langle p, x\rangle - \|x\|^2/2 = (\|p\|^2 - \|p-x\|^2)/2$. The graph of f_x is a hyperplane in $\mathbb{R}^{d+1}$ that is tangent to the paraboloid $\{(p,z) \in \mathbb{R}^d \times \mathbb{R} \mid z \geq \|p\|^2/2\}$. The collection of such hyperplanes decomposes $\mathbb{R}^{d+1}$ into convex cells, which we call the *hyperplane arrangement* of X, denoted $\mathrm{Arr}(X)$; see Figure 2. The *cells* in the arrangement are non-empty intersections of hyperplanes and closed half-spaces. More formally, for each cell there is a three-partition $X = X_{in} \cup X_{on} \cup X_{out}$ such that the cell consists of all point $(p,z) \in \mathbb{R}^d \times \mathbb{R}$ that satisfy

$$z \leq f_x(p) \quad \text{if } x \in X_{in}, \tag{1}$$
$$z = f_x(p) \quad \text{if } x \in X_{on}, \tag{2}$$
$$z \geq f_x(p) \quad \text{if } x \in X_{out}. \tag{3}$$

Since X is assumed to be in general position, the dimension of the cell is $i = d + 1 - |X_{on}|$. Turning the non-strict into strict inequalities, we get the interiors of the cells, which partition $\mathbb{R}^{d+1}$. We refer to the i-dimensional cells as *i-cells* and to the $(d+1)$-cells as *chambers*.

Importantly, there is a bijection between the cells of $\mathrm{Arr}(X)$ and the spherical pairs of X, and therefore also the rhomboids in $\mathrm{Rho}(X)$. To see this, map a point (p,z) in the interior of a cell to the sphere S with center p and squared radius $r^2 = \max\{0, \|p\|^2 - 2z\}$. Using the definition of f_x, we observe that $\mathrm{In}(S) = X_{in}$ and $\mathrm{On}(S) = X_{on}$. We can reverse the map, and while this will not reach the points with $\|p\|^2 - 2z < 0$, these points all belong to the

chamber of the empty spherical pair. This establishes the bijection between the cells and the rhomboids. This bijection reverses dimensions and preserves incidences, which justifies that we call it a *duality* between the rhomboid tiling and the hyperplane arrangement. This completes the proof of Claim 1 in Theorem 1.

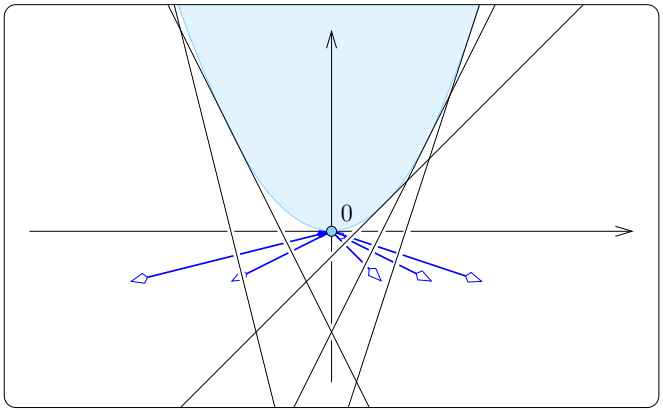

Figure 2 A portion of the arrangement formed by the lines (hyperplanes) tangent to the paraboloid and normal to the vectors $y_x = (x, -1)$. The topmost chamber contains the paraboloid.

Proof of Claim 3: Delaunay mosaics. We begin with some definitions. The *Voronoi domain* of $Q \subseteq X$ is $\text{dom}(Q) = \{p \in \mathbb{R}^d \mid \|p - x\| \leq \|p - y\|, \forall x \in Q, \forall y \in X \setminus Q\}$. Its *order* is $|Q|$. For each Voronoi domain, there is a chamber in $\text{Arr}(X)$ that projects vertically to the domain. Indeed, the chamber is defined by the three-partition $X = X_{in} \cup X_{on} \cup X_{out}$ with $X_{in} = Q$ and $X_{on} = \emptyset$. For each positive integer k, the *order-k Voronoi tessellation* is $\text{Vor}_k(X) = \{\text{dom}(Q) \mid |Q| = k\}$. We can construct it by projecting all chambers whose three-partitions satisfy $|X_{in}| = k$ and $|X_{on}| = 0$. These chambers correspond to the vertices of the rhomboid tiling at depth k. Since $\text{Rho}(X)$ is dual to $\text{Arr}(X)$, we get the dual of the Voronoi tessellation by taking the slice $z = -k$ of $\text{Rho}(X)$. It is therefore convenient to define the *order-k Delaunay mosaic*, denoted $\text{Del}_k(X)$, as the collection of sliced rhomboids at depth k. This completes the proof of Claim 3 in Theorem 1.

We see that the cells of $\text{Del}_k(X)$ are special slices of the rhomboids. Combinatorially, they are equivalent to the diagonal slices of the unit cube that pass through non-empty subsets of the vertices. For the $(d+1)$-cube, there are $d+2$ such slices, which we index from 0 to $d+1$. The j-th slice passes through $\binom{d+1}{j}$ vertices, so we have a vertex for $j = 0, d+1$ and a d-simplex for $j = 1, d$. To describe these slices in general, let U_{d+1} be the $d+1$ unit coordinate vectors. The j-th slice is the convex hull of the points $y_Q = \sum_{u \in Q} u$ with $Q \in \binom{U_{d+1}}{j}$, using $y_\emptyset = 0$ as a convention. To get an intuition, it might be easier to divide the sums by j, in which case the j-th slice is the convex hull of the barycenters of the $(j-1)$-faces of the standard d-simplex; see Figure 3.

3 Multi-covers

In this section, we exploit the rhomboid tiling to shed light on the filtration of multi-covers we get by varying the radius. The main new insight is that the discrete function on the

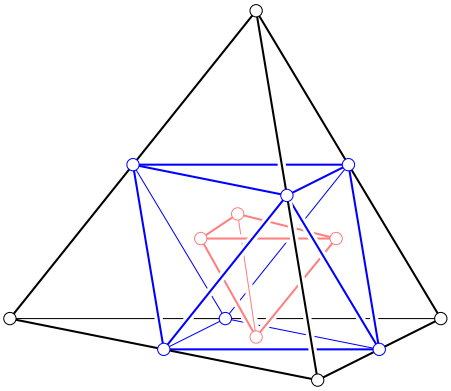

Figure 3 The convex hulls of the barycenters of the $(j-1)$-faces of the tetrahedron. From *outside in*: the tetrahedron for $j = 1$, the octahedron for $j = 2$, and another tetrahedron for $j = 3$.

Delaunay mosaic that encodes this filtration is a relaxation of a standard discrete Morse function. We begin with a formal introduction of the multi-covers.

k-fold cover. Let $X \subseteq \mathbb{R}^d$ be locally finite. Given a radius $r \geq 0$, the *k-fold cover* of X and r consists of all points $p \in \mathbb{R}^d$ for which there are k or more points $x \in X$ with $\|x - p\| \leq r$, or in other words, the points $p \in \mathbb{R}^d$ which are covered by at least k of the balls of radius r around the points $x \in X$. Denoting this set by $\text{Cover}_k(X, r)$, we have

$$\text{Cover}_k(X, r) \subseteq \text{Cover}_k(X, s), \tag{4}$$
$$\text{Cover}_k(X, r) \subseteq \text{Cover}_\ell(X, r), \tag{5}$$

whenever $r \leq s$ and $\ell \leq k$. We are interested in computing the persistent homology of the multi-covers, both in the direction of increasing radius and in the direction of decreasing order. To do so, we represent the covers by complexes, namely by subcomplexes of the Delaunay mosaics. Varying the radius, we get a nested sequence of subcomplexes of the order-k Delaunay mosaic, and the persistent homology can be computed with standard methods; see e.g. [8, Chapter VII]. Varying the order, on the other hand, we get subcomplexes of different Delaunay mosaics, and we need a novel algorithm to compute persistent homology.

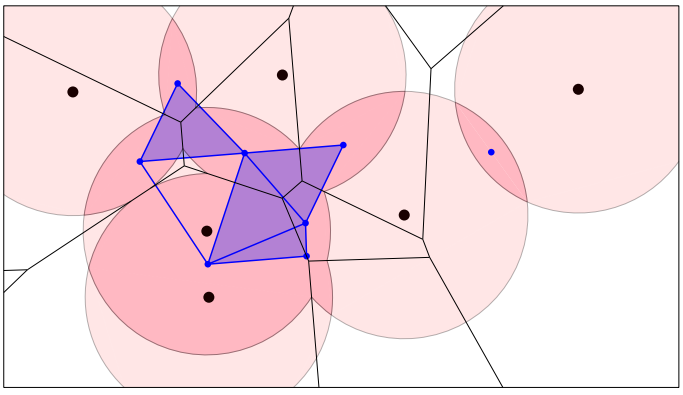

Figure 4 Six points in the plane and a pink ball of radius r centered at each. The black order-2 Voronoi tessellation decomposes the 2-fold cover into convex pieces. The corresponding subcomplex of the dual order-2 Delaunay mosaic is superimposed in blue.

Before we discuss this algorithm in Section 4, we note that the order-k Voronoi tessellation decomposes the k-fold cover into convex sets. To see this, let $|Q| = k$ and define $\mathrm{dom}(Q, r) = \mathrm{dom}(Q) \cap \mathrm{Cover}_k(Q, r)$, which is an intersection of convex sets and therefore convex. We write $\mathrm{Vor}_k(X, r)$ for the collection of domains $\mathrm{dom}(Q, r)$ with $|Q| = k$, and since $\mathrm{dom}(Q, r) = \mathrm{dom}(Q) \cap \mathrm{Cover}_k(X, r)$, we refer to this as the *Voronoi decomposition* of $\mathrm{Cover}_k(X, r)$. Since $\mathrm{dom}(Q, r) \subseteq \mathrm{dom}(Q)$, the dual of this decomposition is a subcomplex of the order-k Delaunay mosaic, which we denote $\mathrm{Del}_k(X, r) \subseteq \mathrm{Del}_k(X)$. See Figure 4 for an example.

▶ **Lemma 2** (Almost Nerve). *Let $X \subseteq \mathbb{R}^d$ be locally finite and in general position. For every integer $k \geq 1$ and real $r \geq 0$, $\mathrm{Del}_k(X, r)$ and $\mathrm{Cover}_k(X, r)$ have the same homotopy type.*

Proof. Recall that the sets $\mathrm{dom}(Q, r)$ with $|Q| = k$ form a convex cover of $\mathrm{Cover}_k(X, r)$. The *nerve* of this collection consists of all sub-collections with non-empty common intersections. By the classic Nerve Theorem [17], this nerve has the same homotopy type as $\mathrm{Cover}_k(X, r)$. This nerve differs from $\mathrm{Del}_k(X, r)$ only in that non-simplicial polytopes of the Delaunay mosaic are now represented by simplices on the same vertex set. We save space by omitting the details to resolve this issue. ◀

The radius function on the rhomboid tiling. To shed additional light on the subcomplexes of the Delaunay mosaics, we introduce a discrete function on the collection of rhomboids discussed in Section 2. Calling it the *radius function*, $\mathcal{R}\colon \mathrm{Rho}(X) \to \mathbb{R}$, we define it by remembering that each j-dimensional rhomboid, $\rho \in \mathrm{Rho}(X)$, corresponds to an $(d + 1 - j)$-dimensional cell, $\rho^* \in \mathrm{Arr}(X)$. Decomposing a point of the cell into its projection to $\mathbb{R}^d$ and the $(d+1)$-st coordinate, we write $q = (p, z) \in \mathbb{R}^d \times \mathbb{R}$, and we define $r_\square(q) = \|p\|^2 - 2z$. With this notation, we define the radius function by mapping ρ to the minimum value of any point in its dual cell:

$$\mathcal{R}(\rho) = \min_{q \in \rho^*} r_\square(q). \tag{6}$$

By convention, the value of the vertex that corresponds to the empty spherical pair is $\mathcal{R}(0) = -\infty$. To obtain a geometric interpretation of this definition, consider the paraboloid defined by the equation $z = \frac{1}{2}\|p\|^2$ in $\mathbb{R}^{d+1}$ and introduce $\pi_t(p)\colon \mathbb{R}^d \to \mathbb{R}$ defined by $\pi_t(p) = \frac{1}{2}(\|p\|^2 - t)$. The image of π_t is the original paraboloid dropped vertically down by a distance $\frac{t}{2}$. With this notation, $\mathcal{R}(\rho)$ is the minimum t such that the image of π_t has a non-empty intersection with ρ^*.

Clearly, $\mathcal{R}$ is *monotonic*, that is: $\mathcal{R}(\rho) \leq \mathcal{R}(\varrho)$ if ρ is a face of ϱ. Indeed, if ρ is a face of ϱ, then ϱ^* is a face of ρ^*, which implies that the paraboloid touches ρ^* at the same time or before it touches ϱ^* when dropped. It follows that the sublevel sets of the radius function are subcomplexes of the rhomboid tiling. For X in general position, the radius function satisfies the stronger requirement of a generalized discrete Morse function; see [12, 13]. To explain what this means, we consider the level sets of a function $f\colon \mathrm{Rho}(X) \to \mathbb{R}$ and define a *step* of $f^{-1}(r)$ as a component in the corresponding Hasse diagram. We call f a *generalized discrete Morse function* if each step is an *interval*, meaning there are rhomboids $\rho \subseteq \varrho$ such that the step consists of all rhomboids that are faces of ϱ and contain ρ as a face. It is useful to distinguish between *singular intervals*, when $\rho = \varrho$, and *non-singular intervals*, when ρ is a proper face of ϱ. Indeed, consider two contiguous sublevel sets, which differ by a level set: $f^{-1}[-\infty, r] \setminus f^{-1}[-\infty, r) = f^{-1}(r)$. If this difference is a non-singular interval, then the two sublevel sets have the same homotopy type, while if the difference is a singular interval, then they have different homotopy types. We prove that the radius function is a generalized discrete Morse function with the special property that every sublevel set is contractible.

▶ **Lemma 3** (Generalized Discrete Morse). *Let $X \subseteq \mathbb{R}^d$ be locally finite and in general position. Then $\mathcal{R}\colon \mathrm{Rho}(X) \to \mathbb{R}$ is a generalized discrete Morse function. Furthermore, all intervals in the implied partition have a vertex as a lower bound, and there is only one singular interval, which contains the vertex at the origin.*

Proof. The vertex at the origin corresponds to the empty spherical pair, has radius $\mathcal{R}(0) = -\infty$, and forms a singular interval. Every other interval is defined by a point $q \in \mathbb{R}^{d+1}$ at which the dropping paraboloid first touches a cell of the arrangement. There is one such point on every plane that is a common intersection of hyperplanes forming the arrangement. By general position, all these points are different. Let q belong to an i-plane, which is common to $j = d + 1 - i$ hyperplanes. It belongs to the interior of an i-cell, which is common to 2^j chambers. Exactly one of these chambers has not already been touched before the i-cell. The paraboloid touches this chamber at the same point q and similarly every cell that is a face of this chamber and contains the i-cell as a face. The corresponding rhomboids form an interval of the radius function, with an upper bound of dimension j and a lower bound of dimension 0. We have $1 \leq j \leq d + 1$, which implies that the interval is not singular.

To show that $\mathcal{R}$ is a generalized discrete Morse function, we still need to make sure that intervals in the same level set are separated. By assumption of general position, there is only one level set that contains more than one interval, namely $\mathcal{R}^{-1}(0)$. All its intervals are of the form $[y_x, 0y_x]$, in which x is a point in X, $0 \in \mathbb{R}^{d+1}$ corresponds to the empty spherical pair, and $0y_x$ is the edge that connects 0 with y_x. While these edges all share 0, no two also share the other endpoint. It follows that these intervals are components of the Hasse diagram of the level set, as required. ◀

The radius function on a Delaunay mosaic. Recall that the order-k Delaunay mosaic of X is the horizontal slice of the rhomboid tiling at depth k . In other words, every cell of $\mathrm{Del}_k(X)$ is the horizontal slice of a rhomboid. More formally, for every $\sigma \in \mathrm{Del}_k(X)$ there is a unique lowest-dimensional rhomboid $\rho \in \mathrm{Rho}(X)$ such that $\sigma = \rho \cap P_k$, in which P_k is the horizontal d-plane defined by $z = -k$. For vertices we have $\dim \sigma = \dim \rho = 0$, and for all higher-dimensional cells we have $\dim \sigma = \dim \rho - 1 \geq 1$. The radius function on the order-k Delaunay mosaic, $\mathcal{R}_k\colon \mathrm{Del}_k(X) \to \mathbb{R}$, is simply the restriction of $\mathcal{R}$ to the horizontal slice: $\mathcal{R}_k(\sigma) = \mathcal{R}(\rho)$. Importantly, this definition is consistent with the subcomplexes $\mathrm{Del}_k(X, r) \subseteq \mathrm{Del}_k(X)$ used to represent the k-fold cover of X and r, but this needs a proof.

▶ **Lemma 4** (Delaunay Radius Function). *Let $X \subseteq \mathbb{R}^d$ be locally finite and in general position. For every integer $k \geq 1$ and every real r, we have $\mathrm{Del}_k(X, r) = \mathcal{R}_k^{-1}[-\infty, r]$.*

Proof. Recall that $\pi_t\colon \mathbb{R}^d \to \mathbb{R}$ is defined by $\pi_t(p) = \frac{1}{2}(\|p\|^2 - t)$. The graph of π_t is a paraboloid that intersects $\mathbb{R}^d$ in the sphere with squared radius t. More generally, the paraboloid intersects every d-plane tangent to the graph of π_0 in an ellipsoid whose vertical projection to $\mathbb{R}^d$ is a sphere with squared radius t. Dropping the paraboloid vertically thus translates into growing balls simultaneously and uniformly centered at the points in X. By definition, $\mathcal{R}(\rho)$ is the value t_0 of t for which the paraboloid touches the dual cell, $\rho^* \in \mathrm{Arr}(X)$, for the first time. More formally, the subset of points $q \in \rho^*$ on or above the graph of π_t is empty for all $t < t_0$ and non-empty for all $t \geq t_0$.

Let σ^* be the vertical projection of ρ^* to $\mathbb{R}^d$, which is a polyhedron in $\mathrm{Vor}_k(X)$ iff its dual cell, σ, belongs to $\mathrm{Del}_k(X)$. Equivalently, $\sigma^* \in \mathrm{Vor}_k(X)$ iff $\mathcal{R}_k(\sigma)$ is defined. By construction, $\sigma^* \cap \mathrm{Cover}_k(X, r)$ is empty for all $r < r_0$ and non-empty for all $r \geq r_0$, in which $r_0^2 = t_0$ is the threshold for σ. By definition, σ belongs to $\mathrm{Del}_k(X, r)$ iff this intersection is non-empty, which implies $\mathrm{Del}_k(X, r) = \mathcal{R}_k^{-1}[-\infty, r]$ for all $r \in \mathbb{R}$, as required. ◀

These results facilitate the computation of the persistence of the k-fold covers for varying radius. Lemma 2 asserts that we can use $\mathrm{Del}_k(X,r)$ as a proxy for $\mathrm{Cover}_k(X,r)$. Lemma 4 provides the recipe for computing the radii of the cells of $\mathrm{Del}_k(X)$, and thus the sublevel set filtration of $\mathrm{Del}_k(X)$, whose persistence module is isomorphic to the persistence of $\mathrm{Cover}_k(X,r)$ for varying radius r. Finally, the persistence diagram is obtained from the filtration via the boundary matrix reduction algorithm [8, Chapter VII].

Assuming $X \subseteq \mathbb{R}^d$ is locally finite and in general position, the radius function of the order-1 Delaunay mosaic is known to be a generalized discrete Morse function [3]. This property does not generalize to higher order. Nevertheless, we can still classify the steps of $\mathcal{R}_k$ into critical and non-critical types such that each critical step changes the homotopy type of the sublevel set in a predictable manner, and every non-critical step maintains the homotopy type of the sublevel set. The proof of this claim together with an enumeration of the types of steps can be found in [9].

4 Persistence in Depth

In this section, we develop an algorithm that computes the persistence of the nested sequence of multi-covers (5). We follow the usual strategy of substituting a complex for each cover, but there are complications. Specifically, we represent $\mathrm{Cover}_k(X,r)$ by $\mathrm{Del}_k(X,r)$ and we introduce additional complexes between the order-k and order-$(k-1)$ mosaics to realize the inclusion between the covers.

Half-integer slices. There are generally no simplicial maps connecting $\mathrm{Del}_k(X)$ with $\mathrm{Del}_{k-1}(X)$. To finesse this difficulty, we take the horizontal *half-integer slice* of the rhomboid tiling at depth $\ell = k - \frac{1}{2}$:

$$\mathrm{Del}_\ell(X) = \mathrm{Rho}(X) \cap P_\ell, \tag{7}$$

for $k \geq 1$. Similar to the Delaunay mosaic, the half-integer slice is a regular complex in $\mathbb{R}^d$. Not surprisingly, there is a well-known dual, namely the *degree-k Voronoi tessellation* [10] that decomposes $\mathbb{R}^d$ into maximal convex domains in which every point has the same k-th nearest point in X. Denoting this tessellation as $\mathrm{Vor}_\ell(X)$, we note that it is the superposition of $\mathrm{Vor}_k(X)$ and $\mathrm{Vor}_{k-1}(X)$, and that it can be constructed by projecting the k-th level in $\mathrm{Arr}(X)$ to $\mathbb{R}^d$. Without going into further details, we observe that this level contains every cell of the arrangement whose corresponding three-partition, $X = X_{in} \cup X_{on} \cup X_{out}$, satisfies $|X_{in}| \leq k-1$ and $|X_{in}| + |X_{on}| \geq k$.

Returning to the mosaics, there are natural simplicial maps $\mathrm{Del}_\ell(X) \to \mathrm{Del}_k(X)$ and $\mathrm{Del}_\ell(X) \to \mathrm{Del}_{k-1}(X)$. However, because such maps lead to complications in the persistence algorithm, we use the horizontal slabs of the rhomboid tiling to connect the mosaics via inclusions. To formally define them, write P_ℓ^k for the points in $\mathbb{R}^{d+1}$ that lie on or between P_ℓ and P_k. We define *slab mosaics* as intersections of such slabs with the rhomboid diagram. Analogous to $\mathrm{Del}_k(X,r)$, we also define radius-dependent subcomplexes of these slab mosaics, as well as of half-integer mosaics, as the respective intersections with sublevel sets of the rhomboid diagram:

$$\mathrm{Del}_\ell^k(X,r) = \mathcal{R}^{-1}[-\infty, r] \cap P_\ell^k, \tag{8}$$

$$\mathrm{Del}_{k-1}^\ell(X,r) = \mathcal{R}^{-1}[-\infty, r] \cap P_{k-1}^\ell, \tag{9}$$

$$\mathrm{Del}_\ell(X,r) = \mathcal{R}^{-1}[-\infty, r] \cap P_\ell. \tag{10}$$

The half-integer Delaunay mosaic includes in both slab mosaics, $\mathrm{Del}_k(X,r)$ includes in the first, and $\mathrm{Del}_{k-1}(X,r)$ includes in the second:

$$\mathrm{Del}_\ell(X,r), \mathrm{Del}_k(X,r) \subseteq \mathrm{Del}^k_\ell(X,r), \tag{11}$$
$$\mathrm{Del}_{k-1}(X,r), \mathrm{Del}_\ell(X,r) \subseteq \mathrm{Del}^\ell_{k-1}(X,r), \tag{12}$$

as illustrated in Figure 5. We will use these relations shortly in the computation of the persistence diagram of the filtration of multi-covers (5).

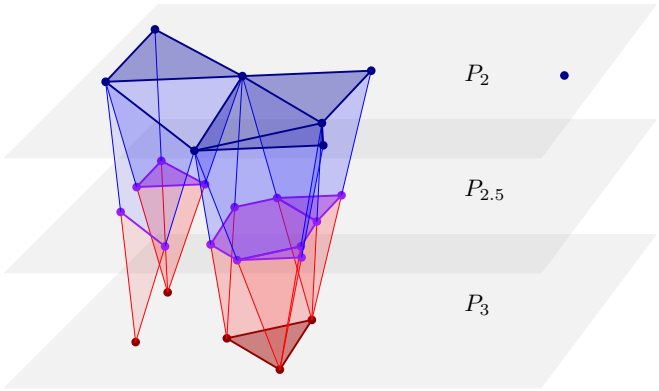

Figure 5 Slices and slabs of the sublevel set $\mathcal{R}^{-1}[-\infty, r]$ of the rhomboid diagram of our previous point set. $\mathrm{Del}_2(X,r)$ in dark blue, $\mathrm{Del}_{2.5}(X,r)$ in purple and $\mathrm{Del}_3(X,r)$ in dark red, with slabs connecting adjacent slices.

Connecting the spaces. To prepare the construction of the persistence and zigzag modules, we connect the multi-covers and the corresponding Delaunay mosaics with maps. Fix $r \geq 0$, let $\ell = k - \frac{1}{2}$, as before, and simplify the notation by writing $C_k = \mathrm{Cover}_k(X,r)$, $D_k = \mathrm{Del}_k(X,r)$, etc. Consider the following diagram with labeled identities and homotopy equivalences:

$$\begin{array}{ccccccccccc}
\longrightarrow & C_k & \xrightarrow{\mathrm{id}} & C_k & \xrightarrow{\mathrm{id}} & C_k & \xrightarrow{\mathrm{id}} & C_k & \longrightarrow & C_{k-1} & \xrightarrow{\mathrm{id}} \\
 & \uparrow{\scriptstyle \mathrm{he}} & & \uparrow{\scriptstyle \mathrm{he}} & & \uparrow{\scriptstyle \mathrm{he}} & & \uparrow{\scriptstyle \mathrm{he}} & & \uparrow{\scriptstyle \mathrm{he}} & \\
\longleftarrow & D_k^{\ell+1} & \xleftarrow{\mathrm{he}} & D_k & \xrightarrow{\mathrm{he}} & D_\ell^k & \xleftarrow{\mathrm{he}} & D_\ell & \longrightarrow & D_{k-1}^\ell & \xleftarrow{\mathrm{he}}
\end{array}$$

The top row stretches out the filtration by writing each multi-cover four times and connecting the copies with the identity. The remaining maps in this row are inclusions.

The bottom row contains all Delaunay mosaics — at integer and half-integer depths — and connects them using the slab mosaics as intermediaries. All maps in this row are inclusions. It is not hard to see that D_k is in fact a deformation retract of D^k_ℓ, as well as a deformation retract of $D^{\ell+1}_k$, which implies that these three have the same homotopy type. It follows that the inclusion maps from an integer Delaunay mosaic to its two incident slab mosaics are homotopy equivalences, as marked in the above diagram.

To define the vertical maps, we first construct the barycentric subdivisions $\mathrm{Sd}\, D_k$ and $\mathrm{Sd}\, D_\ell$ of the Delaunay mosaics, which are simplicial complexes. It suffices to consider the subdivision of D_k. Each vertex $u \in \mathrm{Sd}\, D_k$ represents a j-cell in D_k, which is dual to an i-dimensional Voronoi polyhedron, with $i + j = d$, and we map u to the center of mass of the intersection of this polyhedron with the k-fold cover. By construction, this intersection is non-empty and convex, so it contains the center of mass in its interior. After mapping all

vertices, we map the other simplices of $\operatorname{Sd} D_k$ by piecewise linear interpolation, see Figure 6. It is easy to see that this map is injective, and by Lemma 2, D_k and C_k have the same homotopy type. It follows that the map from D_k to C_k is a homotopy equivalence. The same argument gives a homotopy equivalence from D_ℓ to C_k. The vertical map from D_ℓ^k to C_k is similar, except that we first retract the slab mosaic to its integer boundary, which is D_k, and then we map the barycentric subdivision, as explained above. It follows that all vertical maps are homotopy equivalences.

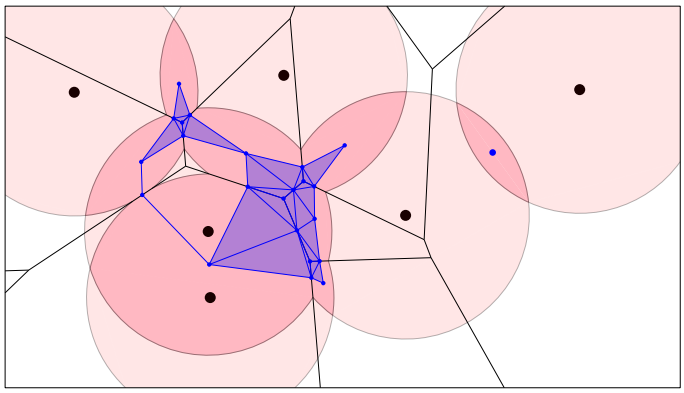

Figure 6 Subdivision of $\mathrm{Del}_2(X, r)$, with its geometric realization inside $\mathrm{Cover}_2(X, r)$.

Modules. Applying the homology functor for a fixed coefficient field, we map all multi-covers and mosaics to vector spaces and all maps to homomorphisms (linear maps) between them. The top row of vector spaces with homomorphisms from left to right is referred to as a *persistence module*, and we denote it $\mathsf{MC}(r)$. The bottom row of vector spaces are connected by homomorphisms that alternate in direction. This kind of structure is referred to as a *zigzag module*, and we denote it $\mathsf{ZZ}(r)$. The advantage of the zigzag module over the persistence module is that its maps are induced by inclusions between complexes, which lend themselves to computations. Our goal, however, is to compute the persistence diagram of $\mathsf{MC}(r)$, and we do this by using $\mathsf{ZZ}(r)$ as a proxy. The following result is therefore essential.

▶ **Lemma 5** (Isomorphism of Modules). *Let $X \subseteq \mathbb{R}^d$ be locally finite and in general position. Then the persistence diagrams of $\mathsf{MC}(r)$ and of $\mathsf{ZZ}(r)$ are the same for every $r \geq 0$.*

Proof. Write C_k and D_k for the vector spaces obtained by applying the homology functor to C_k and D_k, etc. The goal is to show that the diagram of multi-covers and mosaics maps to a diagram of vector spaces in which all squares commute and five sixth of the maps are isomorphisms, as shown:

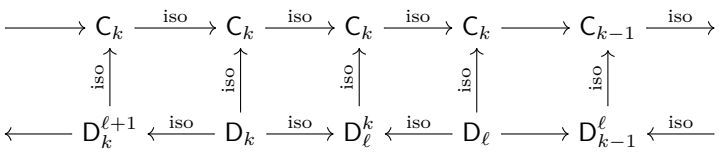

To prove commutativity, we consider the four squares from left to right in the above diagram. The first two squares commute by definition as the inclusion of D_k into each of the adjacent slab mosaics, followed by the corresponding deformation retracting back into D_k, is the identity map.

The third square does not commute before applying the homology functor, but we argue it does after applying the functor. Recall that $\mathrm{Vor}_k(X,r)$ and $\mathrm{Vor}_\ell(X,r)$ are two convex decompositions of C_k and that $\mathrm{Vor}_\ell(X,r)$ is a refinement of $\mathrm{Vor}_k(X,r)$. D_k and D_ℓ are dual to the two Voronoi decompositions. They are generally different, with several vertices of D_ℓ corresponding to one vertex of D_k. When we map $D_\ell \to D_\ell^k \to C_k$, the full subcomplex of these vertices is first contracted to the corresponding single vertex by the deformation retraction from D_ℓ^k to D_k, and second it is mapped to the center of mass of the corresponding domain of $\mathrm{Vor}_k(X,r)$. In contrast, when we map $D_\ell \to C_k$ directly, all these vertices map to different points in C_k, but all these points lie in the interior of the same domain of $\mathrm{Vor}_k(X,r)$. Indeed, the full subcomplex of these vertices is dual to a convex decomposition of this domain and therefore contractible, as all domains are convex sets. It follows that the induced homomorphisms commute. Since there are three isomorphisms in this commuting square, the map from D_ℓ to D_ℓ^k is also an isomorphism, as indicated in the diagram.

The fourth square is similar to the third, with the important difference that the full subcomplex of the set of vertices in D_ℓ that map to a single vertex in D_{k-1} is no longer necessarily contractible. Indeed, we generally do not have isomorphisms from D_ℓ to D_{k-1}^ℓ and from C_k to C_{k-1}. The square still commutes because all non-trivial cycles carried by this subcomplex are killed along $D_\ell \to C_k \to C_{k-1}$ as well as $D_\ell \to D_{k-1}^\ell \to C_{k-1}$.

Isomorphisms are reversible, so we can draw them from left to right in the bottom row of the diagram. The result are two parallel persistence modules whose vector spaces are connected by isomorphisms. The Persistence Equivalence Theorem of persistent homology [8, page 159] implies that the two modules have the same persistence diagram. ◀

Algorithm and running time. We compute the persistence diagram of the filtration of multi-covers (5) using the zigzag algorithm generically described in [4] and explained in detail for inclusion maps in [5]. Its worst-case running time is cubic in the input size, which is the total number of cells in the mosaics. To count the cells, we assume a finite number of points in $\mathbb{R}^d$, $n = |X|$. All cells are horizontal slices or horizontal slabs of rhomboids in $\mathbb{R}^{d+1}$. We therefore begin by counting the rhomboids or, equivalently, the cells in the dual hyperplane arrangement. These numbers are maximized when the n hyperplanes are in general position, and then they depend only on n and d. Observe first that for every $0 \le i \le d+1$, there are $\binom{n}{d+1-i}$ i-planes, each the common intersection of $d+1-i$ hyperplanes. There is one chamber for each plane, which implies that the number of chambers in the arrangement is

$$\Gamma_{d+1}^{d+1}(n) = \binom{n}{d+1} + \binom{n}{d} + \ldots + \binom{n}{0} \le \frac{(n+1)^{d+1}}{(d+1)!}. \tag{13}$$

Indeed, the paraboloid used in the proof of Lemma 3 sweeps out the arrangement and encounters a new chamber whenever it first intersects one of the i-planes, for $0 \le i \le d+1$. The inequality on the right-hand side in (13) is easy to prove, by induction or otherwise. To count the i-cells in the arrangement, we observe that each i-plane carries an arrangement of $n-(d+1-i)$ $(i-1)$-planes. We get the number of (i-dimensional) chambers in this arrangement from (13), and multiplying with the number of i-planes, we get the number of i-cells:

$$\Gamma_i^{d+1}(n) = \binom{n}{d+1-i}\Gamma_i^i(n-d-1+i) \le \frac{n^{d+1-i}}{(d+1-i)!}\frac{(n+1)^i}{i!} \le \frac{(n+1)^{d+1}}{(d+1-i)!\;i!}. \tag{14}$$

Writing $j = d-i$, we get a $(j+1)$-rhomboids in $\mathrm{Rho}(X)$ for every i-cell in the arrangement. In other words, (14) also counts the $(j+1)$-rhomboids in the rhomboid tiling. In particular,

we have $\Gamma^{d+1}_{d+1}(n)$ vertices in the tiling. For $0 \leq j \leq d$, the interior of every $(j+1)$-rhomboid has a non-empty intersection with $2j+1$ hyperplanes P_ℓ, in which 2ℓ is an integer. The $(j+1)$-rhomboid thus contributes $2j+1$ j-cells to the Delaunay mosaics and $2j+2$ $(j+1)$-prisms to the slab mosaics. Taking the sum over all dimensions, we get the total number of cells in the mosaics used in the construction of the zigzag module:

$$\#\text{cells} = \Gamma^{d+1}_{d+1}(n) + \sum_{j=0}^{d}(4j+3)\Gamma^{d+1}_{d-j}(n) \leq \frac{(n+1)^{d+1}}{(d+1)!} + \sum_{i=0}^{d} 4(d{+}1{-}i)\frac{(n+1)^{d+1}}{(d{+}1{-}i)!\; i!} \quad (15)$$

$$\leq \frac{(n+1)^{d+1}}{(d+1)!} + 4(n+1)^{d+1}\sum_{i=0}^{d}\frac{1}{(d-i)!\; i!} \leq 9(n+1)^{d+1}. \quad (16)$$

Taking the third power, we get an upper bound for the worst-case running time of the algorithm and thus the main result of this section.

▶ **Theorem 6** (Multi-cover Persistence). *Let X be a set of n points in general position in $\mathbb{R}^d$. For every radius $r \geq 0$, the persistence diagram of the filtration of multi-covers with radius r can be computed in worst-case time $O(n^{3d+3})$.*

5 Discussion

The main contribution of this paper is the introduction of the $(d+1)$-dimensional rhomboid tiling of a locally finite set of points in $\mathbb{R}^d$. It is the underlying framework that facilitates the study of multi-covers with balls and the computation of the persistence as we increase the radius or we decrease the depth of the coverage. The latter requires novel adaptations of the standard approach to persistence, which for n points in $\mathbb{R}^d$ lead to an algorithm with worst-case running time $O(n^{3d+3})$. This compares favorably to naive solutions and the approach using Čech complexes [21], but it is not practical unless n and d are small. While the time-complexity is too high for the density analysis of large data sets, we see applications in the study of regular or semi-regular configurations that arise in the design and investigation of materials. With some modifications, our results extend to balls with different radii (points with weights). We refrained from discussing this generalization because of the implied loss of intuitive appeal. In particular, Theorem 1 extends, and Theorem 6 holds without change in this more general setting. There are a number of challenging questions raised by the work reported in this paper.

- Instead of computing the persistence in scale and depth separately, it might be interesting to combine both to a concrete setting for 2-parameter persistence [18].
- A set of n points in $\mathbb{R}^d$ has some constant times n^{d+1} spherical pairs. We cannot improve the worst-case time of our persistence in depth algorithm unless we avoid the enumeration of these pairs. Can this be done?

As proved in [1], for every locally finite $X \subseteq \mathbb{R}^d$, there is a locally finite $Y \subseteq \mathbb{R}^d$ with real weights such that the (order-1) weighted Voronoi tessellation of Y is the order-k Voronoi tessellation of X. However, growing balls uniformly with centers in X and growing them according to the weights with centers in Y gives different filtrations of the dual Delaunay mosaic. It would be interesting to quantify this difference by bounding the distance between the two persistence diagrams.

References

1 F. Aurenhammer. A new duality result concerning Voronoi diagrams. *Discrete Comput. Geom.* **5** (1990), 243–254.

2 F. Aurenhammer and O. Schwarzkopf. A simple on-line randomized incremental algorithm for computing higher order Voronoi diagrams. *Int. J. Comput. Geom. Appl.* **2** (1992), 363–381.

3 U. Bauer and H. Edelsbrunner. The Morse theory of Čech and Delaunay complexes. *Trans. Amer. Math. Soc.* **369** (2017), 3741–3762.

4 G. Carlsson and V. de Silva. Zigzag persistence. *Found. Comput. Math.* **10** (2010), 367–405.

5 G. Carlsson, V. de Silva and D. Morozov. Zigzag persistent homology and real-valued functions. *In* "Proc. 25th Ann. Sympos. Comput. Geom., 2009", 247–256.

6 F. Chazal, D. Cohen-Steiner and Q. Mérigot. Geometric inference for measures based on distance functions. *Found. Comput. Math.* **11** (2011), 733–751.

7 H. Edelsbrunner. *Algorithms in Combinatorial Geometry.* Springer-Verlag, Heidelberg, Germany, 1987.

8 H. Edelsbrunner and J.L. Harer. *Computational Topology. An Introduction.* Amer. Math. Soc., Providence, Rhode Island, 2010.

9 H. Edelsbrunner and G. Osang. The topology of a step. Manuscript, IST Austria, Klosterneuburg, Austria, 2017.

10 H. Edelsbrunner and R. Seidel. Voronoi diagrams and arrangements. *Discrete Comput. Geom.* **1** (1986), 25–44.

11 G. Fejes Toth. Multiple packing and covering of the plane with circles. *Acta Math. Acad. Sci. Hung.* **27** (1976), 135–140.

12 R. Forman. Morse theory for cell complexes. *Adv. Math.* **134** (1998), 90–145.

13 R. Freij. Equivariant discrete Morse theory. *Discrete Math.* **309** (2009), 3821–3829.

14 L. Guibas, Q. Mérigot and D. Morozov. Witnessed k-distance. *Discrete Comput. Geom.* **49** (2013), 22–45.

15 D. Krasnoshchekov and V. Polishchuk. Order-k alpha hulls and alpha shapes. *Inform. Process. Lett.* **14** (2014), 76–83.

16 D.T. Lee. On k-nearest neighbor Voronoi diagrams in the plane. *IEEE Trans. Comput.* **C-31** (1982), 478–487.

17 J. Leray. Sur la forme des espaces topologiques et sur les points fixes des représentations. *J. Math. Pures Appl.* **24** (1945), 95–167.

18 M. Lesnick and M. Wright. Interactive visualization of 2-D persistence modules. arXiv 1512.00180, 2015.

19 K. Mulmuley. Output sensitive construction of levels and Voronoi diagrams in $\mathbb{R}^d$ of order 1 to k. *In* "Proc. 22nd Ann. ACM Sympos. Theory Comput., 1990", 322–330.

20 M.I. Shamos and D.J. Hoey. Closest-point problems. *In* "Proc. 16th Ann. IEEE Sympos. Found. Comput. Sci, 1975", 151–162.

21 D.R. Sheehy. A multi-cover nerve for geometric inference. *In* "Proc. Canadian Conf. Comput. Geom., 2012".

A Notation

$p, x, x_Q; q, y_x, y_Q$	points in $\mathbb{R}^d$; in $\mathbb{R}^{d+1}$
z, w	$(d+1)$-st, $(d+2)$-nd coordinate
u, v	vectors
$\mu, \bar{\mu}, \nu$	vertices
k, n	order, dimension
$j+1, j; i$	dimension of rhomboid, Delaunay cell; Voronoi polyhedron
$\rho, \varrho; \rho^*, \varrho^*$	rhomboid; dual cell in arrangement
$\sigma, \tau; \sigma^*, \tau^*$	Delaunay cells; dual Voronoi polyhedra
P_k, P_ℓ^k	horizontal hyperplane, slab
f_x, F_x, G_x	affine functions
$I = \mathrm{In}(S), U = \mathrm{On}(S)$	sets inside, on sphere
$U = U_{in} \cup U_{on} \cup U_{out}$	three-partition
$X = X_{in} \cup X_{on} \cup X_{out}$	three-partition
$Q \subseteq X$	simplex
$X \subseteq \mathbb{R}^d$	locally finite point set
$\mathrm{rho}(I, U)$	rhomboid of spherical pair
$\mathrm{dom}(Q), \mathrm{dom}(Q, r)$	unrestricted, restricted Voronoi domain
$\mathrm{Rho}(X), \mathrm{Arr}(X)$	rhomboid tiling, hyperplane arrangement
$\mathrm{Cover}_k(X, r)$	k-fold cover
$\mathrm{Vor}_k(X), \mathrm{Vor}_k(X, r)$	order-k Voronoi tessellation, decomposition
$\mathrm{Del}_k(X), \mathrm{Del}_k(X, r), \mathrm{Del}_\ell^k(X, r)$	order-k Delaunay mosaic, slab mosaic
$\mathcal{R}\colon \mathrm{Rho}(X) \to \mathbb{R}$	radius functions on rhomboid tiling
$\mathcal{R}_k\colon \mathrm{Del}_k(X) \to \mathbb{R}$	radius functions on Delaunay mosaic
$\mathcal{D}\colon \mathrm{Rho}(X) \to \mathbb{R}$	depth functions on rhomboid tiling
$\pi_t\colon \mathbb{R}^d \to \mathbb{R}$	dropping paraboloid
$r_\square\colon \mathbb{R}^{d+1} \to \mathbb{R}$	time when the paraboloid passes
C_k, D_k, D_ℓ^k	short-forms for cover, Delaunay mosaic, slab mosaic
$\mathsf{C}_k, \mathsf{D}_k, \mathsf{D}_\ell^k$	vector spaces after homology functor
$\Gamma_i^{d+1}(n)$	number of i-cells in arrangement

Table 1 Notation for concepts, sets, functions, vectors, variables.

B Definitions and Results

- Section 1: Introduction.
- Section 2: Rhomboid Tiling.
  - Def.: *rhomboid tiling*, $\mathrm{Rho}(X)$.
  - Def.: *order-k Delaunay mosaic*, $\mathrm{Del}_k(X)$.
  - Theorem 1 (Rhomboid Tiling).
- Section 3: Multi-covers.
  - Def.: *k-fold cover*, $\mathrm{Cover}_k(X, r)$.
  - Def.: *radius functions*, $\mathcal{R}\colon \mathrm{Rho}(X) \to \mathbb{R}$, $\mathcal{R}_k\colon \mathrm{Del}_k(X) \to \mathbb{R}$.
  - Lemma 2 (Almost Nerve).
  - Lemma 3 (Generalized Discrete Morse).
  - Lemma 4 (Delaunay Radius Function).
- Section 4: Persistence in Depth.
  - Def.: *half-integer slice*, $\mathrm{Del}_\ell(X, r)$, *half-integer slab*, $\mathrm{Del}^k_\ell(X, r)$.
  - Def.: *persistence module*, $\mathsf{MC}(r)$, *zigzag module*, $\mathsf{ZZ}(r)$.
  - Lemma 5 (Isomorphism of Modules).
  - Theorem 6 (Multi-cover Persistence).

C To do or think about

- Section 1: Introduction.
- Section 2: Rhomboid Tiling.
- Section 3: Multi-covers.
- Section 4: Persistence in Depth.
- Section 5: Discussion.